Dehalogenation of Iodinated X-ray Contrast Media in a Bioelectrochemical System

ARTICLE *in* ENVIRONMENTAL SCIENCE & TECHNOLOGY · JANUARY 2011

Impact Factor: 5.33 · DOI: 10.1021/es1022812 · Source: PubMed

Environ. Sci. Technol. **2011,** *45,* 782–788

Dehalogenation of Iodinated X-ray Contrast Media in a Bioelectrochemical System

YANG MU,*,† JELENA RADJENOVIC,† JINYOU SHEN,†,‡ RENÉ A. ROZENDAL,† KORNEEL RABAEY,† AND JÜRG KELLER†

Advanced Water Management Centre, The University of Queensland, St. Lucia, QLD 4072, Australia, School of Chemical Engineering, Nanjing University of Science and Technology, 200 Xiaolingwei Street, Nanjing 210094, Jiangsu Province, People's Republic of China

Received July 7, 2010. Revised manuscript received November 10, 2010. Accepted November 19, 2010.

Iodinated X-ray contrast media (ICM) are only to a limited extent removed from conventional wastewater treatment plants, due to their high recalcitrance. This work reports on the cathodic dehalogenation of the ICM iopromide in a bioelectrochemical system (BES), fed with acetate at the anode and iopromide at the cathode. When the granular graphite cathode potential was decreased from −500 to −850 mV vs standard hydrogen electrode (SHE), the iopromide removal and the iodide release rates increased from 0 to 4.62 ± 0.01 mmol m^{-3} TCC d^{-1} and 0 to 13.4 ± 0.16 mmol m^{-3} TCC d^{-1} (Total Cathodic Compartment, TCC) respectively. Correspondingly, the power consumption increased from 0.4 ± 1 to 20.5 ± 3.3 W m^{-3} TCC. The Coulombic efficiency of the iopromide dehalogenation at the cathode was less than 1%, while the Coulombic efficiency of the acetate oxidation at the anode was lower than 50% at various granular graphite cathode potentials. The results suggest that iopromide could be completely dehalogenated in BESs when the granular graphite cathode potential was controlled at −800 mV vs SHE or lower. This finding was further confirmed using mass spectrometry to identify the dehalogenated intermediates and products of iopromide in BESs. Kinetic analysis indicates that iopromide dehalogenation in batch experiments can be described by a first-order model at various cathode potentials. This work demonstrates that the BESs have a potential for efficient dehalogenation of ICM from wastewater or environmental streams.

Introduction

Iodinated X-ray contrast media (ICM), such as iopromide (IPM), are frequently applied in clinical diagnosis to image soft tissues like blood vessels, organs, and lacunae (*1*). The annual worldwide consumption of ICM in X-ray diagnostics is around 3000 tons (*1*). Due to their recalcitrance, ICM are hardly removed by wastewater treatment plants and are consequently discharged in receiving waters (*2*). For example, effluent concentrations of up to 21 μg L^{-1} IPM have been found in rivers and lakes (*2, 3*). Although ICM are believed to be harmless (*4*), subtle effects of mixtures of ICM with their metabolites and other micropollutants are unknown and may exert unanticipated ecological or human health risks (*5*). Given their very low biodegradability, they may also accumulate in the environment (*4*).

Due to high oxidation resistance of the tri-iodinated aromatic ring structure, ICM have been reported to only loose their alkyl side chains by biological and chemical oxidation (*6*). Advanced oxidation processes (AOPs) have been suggested as an innovative technology for ICM removal. However, treatment of ICM with AOPs might be inefficient because the generated OH radicals react nonselectively with many nontarget water constituents as well, including natural organic matter and bicarbonate (*6*). As an alternative treatment, ICM can also be reductively dehalogenated by zerovalent iron, but the deiodination is not complete (*7*).

Electrochemical reduction of halogenated compounds has recently received growing attention, due to its selectivity, versatility, and environmental compatibility (*8*). However, information about electrochemical dehalogenation of ICM is very limited, and so far only one study has been published on the electrochemical dehalogenation of the ICM iomeprol (*9*). Moreover, in the latter study, chemical catalysts were used in both anode (platinum net) and cathode (reticulated nickel foam electrode) in order to reduce the overpotentials, i.e., decrease the power consumption of the electrochemical cell.

Recently, bioelectrochemical systems (BESs), such as microbial fuel cells (MFCs) and microbial electrolysis cells (MECs), have been explored extensively for their innovative features and environmental benefits (*10*). At the anode, organic material from the wastewater is oxidized by electrochemically active microorganisms. Subsequently, the microorganisms transfer the electrons resulting from this oxidation to the anode via extracellular electron transfer. Through an electrical circuit, the electrons are transported to the cathode, where they are consumed for oxygen reduction (in the case of MFCs) or hydrogen formation (in the case of MECs). The overpotential could be significantly reduced by the electrochemically active bacteria at the anode and/or cathode, thus cheap materials such as graphite and carbon could be chosen as electrodes in BESs (*10*). In addition, the oxidative and reductive capacities of BESs have been demonstrated through a plethora of valuable applications in previous studies. For example, BESs have been applied to remove organic and inorganic contaminants such as acetate (*11*), cellulose (*12*), rhizodeposits of rice plants (*13*), and sulfur (*14*) from wastewater at the anode chamber. However, BESs can reduce nitrate and nitrobenzene (*15, 16*), reductively dehalogenate (*17*), and decolourize azo dyes (*18*) at the cathode.

Here, we report for the first time the reductive dehalogenation of ICM at the cathode of a BES, driven by microbial oxidation of organics at the anode. Nonionic IPM was chosen as a model ICM compound. The focus of this work was on the process feasibility, Coulombic efficiency and kinetics, as well as the identification of the dehalogenation intermediates and products.

Materials and Methods

Chemical Reagents. IPM (USP reference standard) and sodium acetate (analytical grade) were purchased from Merck Pty Limited (Kilsyth Victoria, Australia) and Sigma-Aldrich (Sydney, Australia), respectively. The chemical structure of IPM is shown in Figure 1. The reverse osmosis concentrate

* Corresponding author phone: +61 7 3346 3218; fax: +61 7 3365 4726; e-mail: yangmu@awmc.uq.edu.au.

† Advanced Water Management Centre, The University of Queensland.

‡ School of Chemical Engineering, Nanjing University of Science and Technology.

10.1021/es1022812
Published on Web 12/08/2010

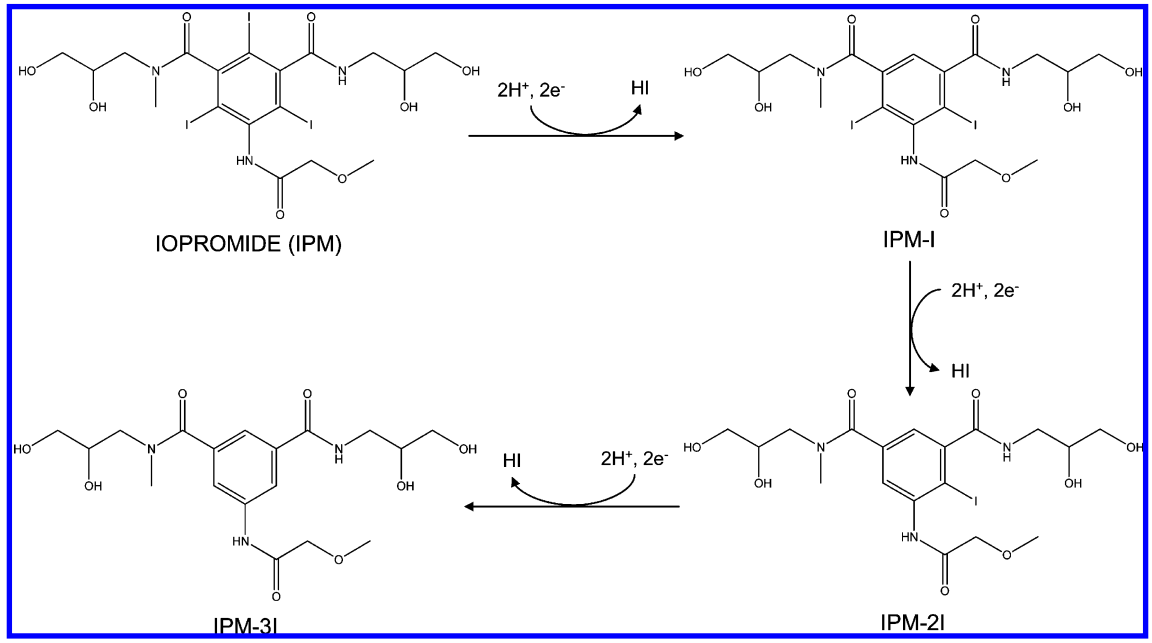

FIGURE 1. Possible pathway for IPM dehalogenation at granular graphite cathode potential of −800 mV vs SHE in BESs.

TABLE 1. IPM Removal from a Reverse Osmosis Concentrate in the BES at the Granular Graphite Cathode Potential −800 mV vs SHE (Cathode HRT = 3.64 h, Number of Measurements for the Standard Deviation *n* = 3)

	cathode influent	cathode effluent after 7 days	cathode effluent after 3 months
IPM (μg L^{-1})	12 ± 3	0	0.3 ± 0.2
pH	7.8 ± 0.1	9.0 ± 0.1	9.1 ± 0.2
TOC (mg L^{-1})	64.8 ± 6	65.0 ± 4.8	63 ± 8
COD (mg L^{-1})	166 ± 15	170 ± 4	165 ± 10
Color (mg L^{-1})	146 ± 10	143 ± 13	140 ± 10

was collected from the Bundamba Advanced Water Treatment Plant in Queensland, Australia and its characteristics are shown in Table 1. The IPM concentration in the reverse osmosis concentrate was about 0.015 ± 0.004 μmol L^{-1} (12 ± 3 μg L^{-1}) without any addition.

Bioelectrochemical System. The BES was constructed by assembling two equal rectangular Perspex frames with internal dimensions of 0.14 × 0.12 × 0.02 m. The frames were bolted together between two Perspex square plates. A cation exchange membrane (Ultrex CMI-7000, Membranes International, U.S.A.) was placed between the anode and the cathode. Sealing was ensured by rubber gaskets inserted between each frame. The total empty volume for each compartment was 336 mL (Total Cathodic Compartment, TCC). The anodic start-up procedure of the BES can be found from our previous studies (*16, 18*). Granular graphite with diameter ranging from 2 to 6 mm (El Carb 100, Graphite Sales, Inc., U.S.A.) was used as electrode in both the anode and cathode compartments, reducing the compartment liquid volume to 182 mL. Prior to use, graphite granules were pretreated with acid and base to eliminate any potentially catalytic foreign compounds from the graphite surface. At first, granules were kept in 1 mol L^{-1} HCl for 24 h and then washed 4−5 times with water. After that granules were kept in 1 mol L^{-1} NaOH solution for 24 h and finally washed 8−10 times again with water. By killing all microorganisms, this treatment also eliminated any potential biocatalyst that could have affected the cathode performance. To ensure that biological activity would not influence the results, the experiments were started immediately after adding the pretreated granules to the reactor. The fact that the cathode performance was established very quickly and did not change over time strongly indicates that no biocatalysis was developing during the operation of this reactor. The graphite rod contacts of both anode and cathode and the reference electrode were connected to a potentiostat (VMP3 multichannel potentiostat, Princeton Applied Research, U.S.A.) for cathodic potential control.

During the startup, the anodic compartment of the BES was inoculated with a microbial consortium previously enriched in MFCs (*19*) with acetate as the carbon source, and continuously fed with a modified M9 medium as described previously (*20*). Throughout all of the experiments, a growth medium with 320 mg L^{-1} sodium acetate, i.e., 250 mg L^{-1} COD (chemical oxygen demand) as electron donor was continuously fed to the anode compartment at a flow rate of 540 mL d^{-1}. Both the anolyte and catholyte were recirculated at a rate of ∼200 mL min^{-1} to maintain well-mixed conditions and to avoid concentration gradients. The cathodic half-cell potentials were measured by placing an Ag/AgCl reference electrode (assumed +0.197 V vs SHE) (ref 201, BioAnalytical Systems) in the cathode compartment of each BES. All experiments were performed 24 ± 2 °C.

Continuous Cathode Experiments. The experimental setup for continuous cathode experiments is shown in Figure S1(A) of the Supporting Information (SI). The BES was first operated in an open circuit to confirm that IPM dehalogenation was not associated with absorption into the graphite material or with the catalytic activity of the graphite material. Then the circuit of the BES was closed and a series of experiments were conducted in order to investigate the influence of various operational parameters on IPM dehalogenation. The variations in the operational parameters are listed in Table S1 of the SI. As our preliminary experiments suggested that IPM could not be dehalogenated when the cathode potential was −500 mV vs SHE or higher, the granular graphite cathode potential was decreased from −500 to −850 mV vs standard hydrogen electrode (SHE) in series 1. As the IPM concentration was found to be at different levels in wastewater or environmental streams (*3*), the cathode feed consisted of either a high (1.31 μmol L^{-1}) or a low (0.0145 μmol L^{-1}) concentration of IPM with a 50 mmol L^{-1} phosphate buffer (pH 7). In order to set cathode pH at different levels in series 2, the cathode feed was prepared without phosphate buffer, and its pH was varied using 0.1 mM HCl. Then sodium

chloride was dosed into the cathode feed to keep the solution conductivity at a similar level of about 4.0 mS cm^{-1}. In series 3, the different dissolved oxygen (DO) levels in the cathode feed were set by varying the flow rate of the aeration with a flow rotameter. In order to keep the DO concentrate at zero in series 1, 2, and 3, the cathode feed was sparged with nitrogen gas to remove oxygen. Throughout the continuous experiments, the cathode flow rate was controlled at 50 mL h^{-1}, resulting in a hydraulic retention time (HRT) of 3.64 h at the cathode.

A comparison experiment was operated with a 0.1 × 0.1 m boron-doped diamond (BDD) mesh cathode (Magneto Special Anodes B. V., Holland) and the cathode potential was controlled in the range of −500 to −1000 mV vs SHE. The BDD cathode feed consisted of a 50 mmol L^{-1} phosphate buffer (pH 7) with 1.31 μmol L^{-1} of IPM with sparging nitrogen. Each experiment lasted one week to ensure that the reactor reached steady-state; this was assessed based on constant IPM removal and/or iodide release rates. Only those results obtained under steady-state conditions are reported here. Lastly, in order to investigate the dehalogenation efficiency of BESs for a real wastewater, the granular graphite cathode was fed with reverse osmosis concentrate containing IPM and the cathode potential was controlled at −800 mV vs SHE for running about three months, and the reverse osmosis concentrate was sparged with nitrogen before feeding.

Batch Cathode Experiments. The experimental setup for batch cathode experiments is shown in Figure S1(B) of the SI. An external bottle of 2 L was used in the cathodic recirculation line during batch experiments. As it was found from continuous cathode experiments that IPM could not been dehalogenated when the cathode potential was −500 mV vs SHE or higher, the granular graphite cathode potential was controlled at −600, −700, and −800 mV SHE, respectively, using a potentiostat to investigate the IPM dehalogenation kinetics. The cathode feed consisted of a 50 mmol L^{-1} phosphate buffer (pH 7) with 1.31 μmol L^{-1} of IPM, and were sparged with nitrogen gas to remove oxygen. Each experiment was repeated three times.

Chemical Analysis. Samples taken using a 5-mL syringe from both the anode and the cathode were filtered immediately through a 0.22 μm filter. IPM as well as its dehalogenated products were analyzed using Shimadzu Prominence ultrafast liquid chromatography (UFLC) system coupled to a 4000 QTRAP hybrid triple quadrupole-linear ion trap mass spectrometer (QqLIT-MS) equipped with a Turbo Ion Spray source (Applied Biosystems-Sciex, Foster City, CA, U.S.A.). The Turbo Ion Spray source was operated in positive ion (PI) mode using the following settings for the ion source and mass spectrometer: curtain gas 30 psi, spraying gas 62 psi, drying gas 62 psi, drying gas temperature of 700 °C, and ion spray voltage of 5500 V. The declustering potential (DP) and the collision energy (CE) were optimized for each compound and were in the range 120−130 V and 20−45 eV, respectively, while the excitation energy was set to 10 eV. Detailed information on the used DP and CE values is summarized in the captions of Figures S2, S3-1, S3-2, and S3-3 of the SI. Chromatographic separation was achieved with an Alltima C18 Column (250 × 4.6 mm, particle size 5 μm) run at 40 °C, using acetonitrile with 0.1% formic acid as eluent A and HPLC grade water with 0.1% formic acid as eluent B, at a flow rate of 1 mL min^{-1}. The elution started at 5% of A and was linearly increased to 40% of A in 10 min, held isocratically for 4 min and then returned to the initial conditions. The total runtime, including the conditioning of the column to the initial conditions was 18 min. The injection volume of the sample was 20 μL. Iodide release was quantified by ion chromatography with UV detector (Dionex ICS-2000). For acetate analysis, 0.9 mL sample was added to 0.1 mL of 10% formic acid solution and analyzed with a gas chromatography method using a polar capillary column (DB-FFAP) at 140 °C and a flame ionization detector at 250 °C. For the reverse osmosis concentrate, total organic carbon (TOC) was determined using a total organic carbon analyzer (Analytik Jena multi N/C 2100), COD measurements were done according to the dichromate method (*21*), and color was analyzed according to Dwyer et al. (*22*).

Calculations. The IPM removal efficiency (%) and rate (mmol m^{-3} TCC d^{-1}) as well as the iodide release rate (mmol m^{-3} TCC d^{-1}) in the continuous cathode experiments were calculated as follows:

$$\text{IPM removal efficiency} = \frac{C_{\text{inf-IPM}} - C_{\text{eff-IPM}}}{C_{\text{inf-IPM}}} \times 100\% \quad (1)$$

$$\text{IPM removal rate} = \frac{(C_{\text{inf-IPM}} - C_{\text{eff-IPM}}) \times Q_C}{\text{TCC}} \quad (2)$$

$$\text{iodide release rate} = \frac{C_{\text{eff-I}} \times Q_C}{\text{TCC}} \quad (3)$$

where $C_{\text{inf-IPM}}$ and $C_{\text{eff-IPM}}$ are the influent and effluent IPM concentration (μmol L^{-1}) of the cathode respectively, Q_C is the influent flow rate of the cathode (m^3 d^{-1}), TCC is the volume of total cathodic compartment (336×10^{-6} m^3), $C_{\text{eff-I}}$ is the effluent iodide ion concentration (μmol L^{-1}).

The Coulombic efficiency for acetate oxidation at the anode was evaluated according to Logan et al. (*23*). As one mole iodide release from IPM requires two moles of electrons (Figure 1), the Coulombic efficiency on IPM dehalogenation (ε_{IPM}) at the cathode was calculated as follows:

$$\varepsilon_{\text{IPM}} = \frac{2 \times C_{\text{eff-I}} \times \dfrac{Q_C}{24 \times 3600} \times F}{I} \quad (4)$$

where 2 is the number moles of electrons per mole of iodide released, I is the current (mA), and F is Faraday's constant (96 485 C mol^{-1} e).

Results and Discussion

Dehalogenation Performance. IPM removal as a result of absorption into the graphite material or catalytic decomposition at the graphite material was found to be insignificant. During the continuous cathode feeding, both the IPM removal and iodide release were negligible under open circuit conditions (less than 1% IPM removal efficiency), indicating that nonelectrochemical processes for IPM dehalogenation at or adsorption onto the granular graphite electrode surface were minimal. Figure 2 shows the effect of granular graphite cathode potential on the reactor dehalogenation performance in terms of IPM removal and iodide release under closed circuit conditions (pH 7). As shown in Figure 2, the IPM removal efficiency and rate as well as iodide release rate were negligible at a cathode potential of −500 mV vs SHE, which means that the IPM cannot be dehalogenated when the granular graphite cathode potential is −500 mV vs SHE or higher. As the granular graphite cathode potential was decreased from −500 to −850 mV vs SHE (IPM concentration 1.31 μmol L^{-1}), the IPM removal efficiency increased from 0 to 97.6 ± 0.1% (Figure 2A). Correspondingly, the IPM removal and the iodide release rates were increased from 0 to 4.62 ± 0.01 and 13.4 ± 0.01 mmol m^{-3} TCC d^{-1}, respectively (Figure 2B). This suggested that the IPM could be dehalogenated when the granular graphite cathode potential is lower than −500 mV vs SHE. In addition, neither pH nor DO concentration had a significant effect on IPM removal when the cathode potential was controlled at −800 mV vs SHE, i.e., under potentiostatic mode (Figure S5 of the SI). The lack of

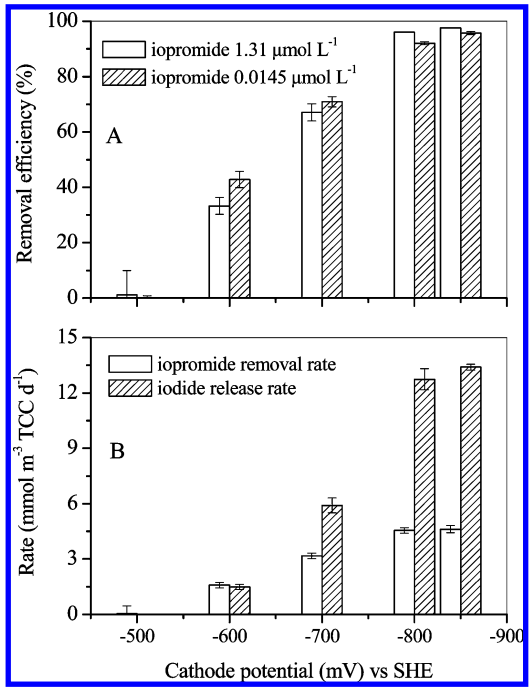

FIGURE 2. Effect of granular graphite cathode potential on (A) IPM removal efficiency at influent IPM concentration 1.31 and 0.0145 μmol L^{-1}, respectively, and (B) IPM removal and iodide release rates at influent IPM concentration 1.31 μmol L^{-1} in BESs (HRT = 3.64 h, cathode pH = 7.0, number of measurements for the standard deviation n = 3).

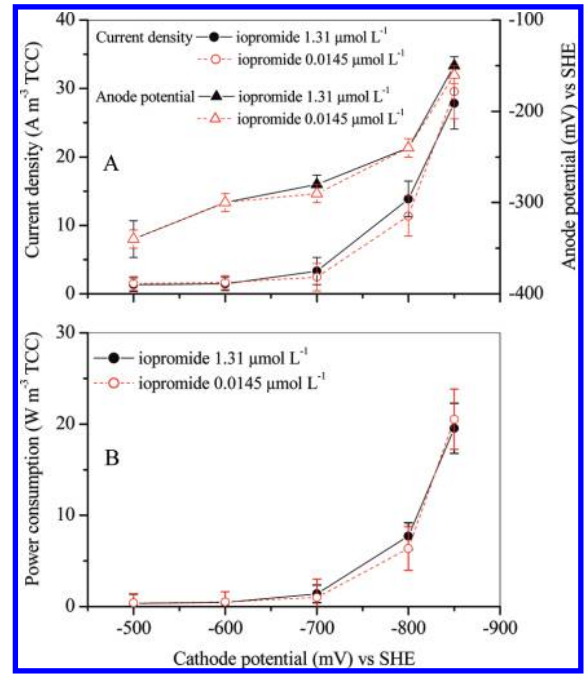

FIGURE 3. Variation of current density, anode potential, and power consumption as a function of the cathode potential at an IPM concentration of 0.0145 μmol L^{-1} and 1.31 μmol L^{-1} (HRT = 3.64 h, cathode pH = 7.0, number of measurements for the standard deviation n = 3).

pH dependence could be due to the fact that IPM is a nonionic compound and sequentially its adsorption on the surface of the granular graphite cathode might be affected slightly by the solution pH. Although oxygen can compete for electrons with IPM at the cathode, this only resulted in a higher current, i.e., more energy consumption at a fixed cathode potential.

In practice, the IPM concentrations such as in the effluent of wastewater treatment plants or in lakes are usually lower than 0.025 μmol L^{-1}, i.e., 20 μg L^{-1} (*1*). Therefore, in order to investigate the effectiveness of the BES for IPM removal at such low concentrations, the experiments were carried out at an influent IPM concentration of about 0.0145 μmol L^{-1}, i.e., 11 μg L^{-1}. As shown in Figure 2A, the IPM removal efficiency was also increased with the decrease of granular graphite cathode potential from −500 to −850 mV vs SHE. When the granular graphite cathode potential was controlled at −850 mV vs SHE, the IPM removal efficiency reached 95.7 ± 0.6%, leaving around 0.5 μg L^{-1} of IPM in the effluent. This result further demonstrates the high efficiency of IPM removal on the granular graphite cathode in the BES, even at such low concentrations. In addition, Figure 2A also suggests that the IPM removal efficiency was independent of the influent IPM concentration in the BES, at least under the experimental conditions tested.

It is also very interesting to note from Figure 2B (IPM concentration 1.31 μmol L^{-1}) that the iodide release rate was similar to the IPM removal rate when the granular graphite cathode potential was at −600 mV vs SHE, and about two times higher when the cathode potential was at −700 mV vs SHE. Finally, when the cathode potential was −800 or −850 mV vs SHE, the iodide release rate was three times higher than the IPM removal rate. As IPM contains three iodide atoms in its structure (Figure 1), these results imply that IPM could be completely dehalogenated at a cathode potential of −800 mV vs SHE or lower, while only releasing one or two iodides when the cathode potential was controlled at −600 or −700 mV vs SHE respectively, in continuous experiments with a cathode HRT of 3.64 h.

In order to reduce hydrogen production at the cathode, we replaced the granular graphite cathode by a BDD electrode, which has a very high overpotential for hydrogen formation (*24*). Although hydrogen production was significantly reduced at the BDD cathode (by around 90%), the IPM removal efficiency was much lower at this cathode (Figure S6 of the SI) compared to the graphite cathode (Figure 2A). The IPM dehalogenation was insignificant at the BDD cathode with the potential of −700 mV vs SHE or higher. At the BDD cathode with the potential of −800 mV vs SHE, the IPM removal efficiency was only 46.8 ± 6.0% (Figure S6 of the SI). Even when the BDD cathode potential was decreased to −1000 mV vs SHE, the IPM removal efficiency was only 80.5 ± 4.4% and iodide mass balance calculation indicated that the IPM could not be completely dehalogenated. The better dehalogenation performance for the granular graphite cathode could be due to a much higher surface area of graphite granules (~8.9 × 10^5 m^2 m^{-3} cathode), compared to the BDD electrode with chemical catalyst (less than 30 m^2 m^{-3} cathode). In addition, the BDD electrode is much more expensive than the graphite granules cathode, which further restricts its application, particularly for wastewater treatment.

Electrochemical Performance. The variation of current density, anode potential as well as power consumption was monitored at various cathode potentials during the IPM dehalogenation, as shown in Figure 3. When the influent IPM concentration was changed from 1.31 to 0.0145 μmol L^{-1}, the electrochemical performance of the BES including current density, anode potential, and power consumption per cathode volume only changed slightly. This is due to the hydrogen production being the dominant reaction at the cathode in this work, which is also evident from the very low Coulombic efficiencies for IPM dehalogenation at the cathode (Table 2). As the cathode potential was decreased from −500 to −850 mV vs SHE, the current density increased from 1.35 ± 1 to 27.8 ± 3.8 A m^{-3} TCC, and the anode potential increased from −340 ± 20 to −150 ± 10 mV vs SHE (Figure 3A). At open circuit, the anode potential was around −350 mV vs SHE with acetate as substrate in this study.

TABLE 2. Coulombic Efficiency for IPM Dehalogenation[a] (ε_{IPM}) and Acetate Oxidation[b] (ε_{AC}) at Various Granular Graphite Cathode Potentials in the BES (Number of Measurements for the Standard Deviation $n = 3$)

cathode potential (mV vs SHE)	ε_{IPM} (%)	ε_{AC} (%)
−600	0.23 ± 0.03	6.75 ± 1.56
−700	0.38 ± 0.01	11.01 ± 1.12
−800	0.20 ± 0.01	35.87 ± 4.01
−850	0.11 ± 0.01	49.07 ± 1.70

[a] Influent IPM = 1.31 μmol L^{-1}, HRT = 3.64 h, cathode pH = 7.0. [b] Influent acetate = 3.9 mmol L^{-1}, HRT = 7.58 h, anode pH = 7.0.

As the anode potential was higher than the cathode potential in each experiment, a power input was always required as shown in Figure 3B. The power consumption per cathode volume increased from 0.4 ± 1 to 20.5 ± 3.3 W m^{-3} TCC when the cathode potential was decreased from −500 to −850 mV vs SHE. At a cathode potential of −800 mV vs SHE with influent IPM concentration of 1.31 μmol L^{-1}, the power consumption per mole IPM removal was about 41 kWh mol^{-1}. This value is much higher than that in the study of Zwiener et al. (*9*), where the energy consumption for the complete deiodination of 0.1 mmol L^{-1} ICM iomeprol was estimated to be 1.6 kWh mol^{-1}. However, for a dehalogenation experiment with 0.1 mmol L^{-1} IPM at a cathode potential of −800 mV vs SHE in this study (HRT 3.64 h and pH 7.0), the power consumption was estimated about 2 kWh mol^{-1}, which is similar to that observed by Zwiener et al. for an equivalent concentration of ICM. In order to reduce the overpotentials, i.e., decrease the power consumption, Zwiener et al. (*9*) used platinum and nickel as anode and cathode materials, respectively. Although the price is comparable between nickel and granular graphite, the price of platinum is much higher (market prices on 29th October, 2010: $54 200/kg for platinum; $23/kg for nickel; less than $2/kg for the granular graphite). In this work, only noncatalyzed and inexpensive graphite granules were used as both the anode and cathode electrodes, which could significantly reduce the capital cost, compared to the study of Zwiener et al (*9*). The microbial oxidation of acetate at the anode could provide a low anode potential, which would further save energy for the IPM dehalogenation.

Coulombic Efficiencies. The Coulombic efficiency of the IPM dehalogenation was less than 1% at the graphite cathode with the potentials from −600 to −850 mV vs SHE (Table 2). It is believed that hydrogen evolution was the predominant reaction at such a low cathode potential range, given that the theoretical potential for hydrogen production at the cathode is only −414 mV vs SHE and the overpotential of the graphite cathode for hydrogen production is not much higher (*17*). However, hydrogen produced from the cathode is not likely the direct reactant to dehalogenate IPM in this work. Knitt et al. (*6*) have demonstrated that dehalogenation of IPM using H_2 requires noble metals such as palladium or nickel as catalysts to convert H_2 to atomic hydrogen, a powerful reducing agent that reacts with oxidized functional groups. In this work, the granular graphite cathode was pretreated with acid and base to remove any potentially catalytic foreign compounds from the graphite material (*25*). Moreover, even with similar hydrogen production rates at the cathode, the IPM removal efficiency was still significantly lower at the BDD electrode (−1000 mV vs SHE) compared to granular graphite electrode (−850 mV vs SHE). However, the indirect dehalogenation, via electrolytic production of atomic hydrogen, could not represent a possible alternative, as this mechanism is normally observed when operating in protonated solvents on cathodes activated with noble metal particles (e.g., Pd, Ru, Rh, Ir, Au) (*26*). Therefore, a direct electron transfer from granular graphite electrode to IPM for dehalogenation appears to be the main reaction mechanism in this work. However, IPM dehalogenation could likely be enhanced considerably at the cathode if the granular graphite cathode is coated with platinum or nickel, as IPM could then also react indirectly with the cathodically produced hydrogen, which requires further investigation.

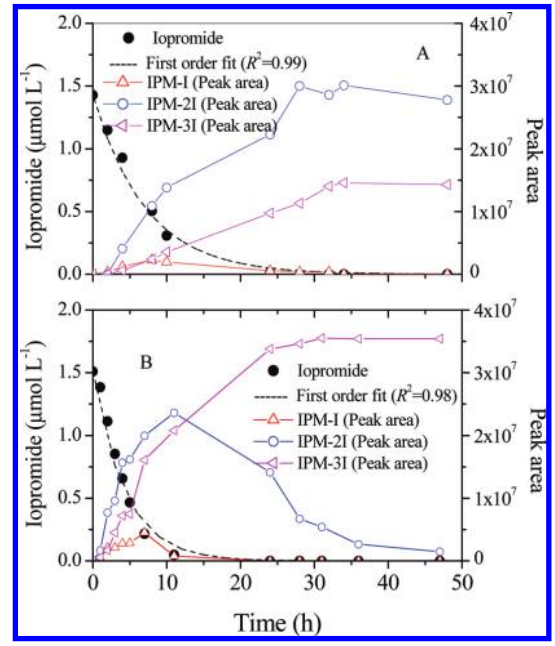

FIGURE 4. Kinetics of IPM dehalogenation in batch experiments at cathode potential (A) −700 mV vs SHE and (B) −800 mV vs SHE, respectively (cathode pH = 7.0). Efficient deiodination of iodinated X-ray contrast media in an abiotic cathodic reaction coupled with a biological anode in a bioelectrochemical system is demonstrated in this work.

As shown in Table 2, the Coulombic efficiency for acetate oxidation at the anode was generally lower than 50%. In this work, the anodic potentials were in the range of −150 to −338 mV vs SHE at various cathode potentials (Figure 3A), which provided the bacteria growing at the anodic electrode surface with very limited energy gain and hence may have favored alternative processes. Acetoclastic methanogenesis and bacterial growth were speculated to both be causes for the low Coulombic efficiencies obtained at the anode. A detailed investigation of these processes in a very similar anode system has been previously undertaken by Freguia et al. (*19*). This demonstrated that further fine-tuning of the anodic potential and loading will allow minimizing these losses and thus increasing the Coulombic efficiency at the anode. In addition, the Coulombic efficiency for acetate oxidation at the anode was increased with the increase in current density (Table 2 and Figure 3A), indicating that electrochemically active bacteria were more active at higher current densities.

Dehalogenation Kinetics in Batch Experiments. IPM dehalogenation in batch experiments can be described by a first-order model at various cathode potentials, and the regression coefficients R^2 were higher than 0.98 (Figure 4). Pseudo first-order rate constants (k_{obs}, h^{-1}) were determined for each batch reaction by fitting a linearized first-order model to the natural log of IPM concentrations measured as a function of time. The k_{obs} values increased from 0 to 0.44 ± 0.11 h^{-1} as the cathode potential was decreased from −500 to −800 mV vs SHE (Figure S7 of the SI). This trend agrees with potential dependent electrode kinetics formulation of

the Butler−Volmer model, where the rate constant is an exponential function of electrode potential in its irreversible form (*27*).

Identification of Reductive Intermediates and Products. In order to identify the intermediates and products of reductive dehalogenation of IPM at the granular graphite cathode in the BES, cathodic sample batch experiments were analyzed using the full-scan mode of the QqLIT-MS instrument. The interpretation of the fragmentation pathways of IPM and its products and their structural elucidation was facilitated in the MS/MS/MS (MS^3) experiments. The whole analysis process for identifying reductive intermediates and products (IPM-I: product which IPM release one iodine; IPM-2I: product which IPM release two iodine; and IPM-3I: product which IPM release three iodine) is provided in the SI. The extracted ion chromatograms (XIC) of IPM, IPM-I, IPM-2I, and IPM-3I are presented in Figure S2 of the SI. The MS^3 experiments revealed similar fragmentation patterns of all four compounds, with typical losses of water and cleavage of secondary amide bond in the side chain, as well as loss of HI in the case of IPM, IPM-I, and IPM-2I (Figures S3-1 to S3-3 of the SI). On the basis of the obtained spectra, fragmentation pathways were proposed as summarized in Figures S4-1 of the SI to 4. The exact position of the iodine cleavage at the aromatic ring could not be determined as in the conducted collision induced dissociation experiments this moiety remained intact.

It should be noted that these intermediates and products could not be quantified due to the unavailability of analytical standards, and were only qualitatively estimated using their normalized peak areas in QqLIT-MS (Figure 4). In the continuous cathodic experiments, IPM-3I was identified as the dominant product when the cathode potential was controlled at −800 mV vs SHE, further confirming that IPM was completely dehalogenated at this cathode potential. In the cathodic batch experiments, the evolution of intermediates and products from the IPM dehalogenation at cathode potentials of −700 and −800 mV vs SHE was monitored, as shown in Figure 4. At a cathode potential of −700 mV vs SHE, the peak area of IPM-I increased to a maximum value at 8 h and then decreased to zero after 34 h. The peak areas of both IPM-2I and IPM-3I reached a maximum value at about 34 h, suggesting that both IPM-2I and IPM-3I were the reductive products of IPM dehalogenation at a cathode potential of −700 mV vs SHE after 34 h batch reaction time. However, the peak area of IPM-2I was decreased after a total reaction time of 50 h. This implies that IPM-2I could eventually be converted to IPM-3I over an extended batch reaction time. At a cathode potential of −800 mV vs SHE, the peak area of both IPM-I and IPM-2I increased to a maximum value (at 7 h for IPM-I and 11 h for IPM-2I) and then decreased to nearly zero (after 11 h for IPM-I and 48 h for IPM-2I) with the increase of reaction time. However, the peak area of IPM-3I continuously increased over the reaction time and reached a maximum value after 48 h. These results indicate that both IPM-I and IPM-2I were the intermediates and IPM-3I was the final product for IPM dehalogenation at a cathode potential of −800 mV vs SHE within 48 h reaction. The proposed pathway for the IPM dehalogenation at the granular graphite cathode in a BES is shown in Figure 1, where IPM is completely dehalogenated through three steps without any further reduction of aldehyde groups, amide bond, or aromatic bonds. However, Zwiener et al. (*9*) observed that a transformation product was formed from the completely dehalogenated iomeprol by a further cleavage of the an amide bond and release of a (C═O)CHOH group from the side chain of iomeprol. Since this breakdown was observed after complete dehalogenation of iomeprol, it is believed that the cleavage of the amide bond should overcome higher bond energy, compared to that of C−I bond, i.e., the release of iodide. As Zwiener et al used nickel foam electrode as cathode, the breakdown of amide bond might be due to the catalytic ability of nickel to overcome higher bond energy, resulting in the formation of a fourth transformation product. However, the graphite cathode used in our work did not include any chemical catalysts, thus likely has a much higher overpotential for the cleavage of the amide bond. Therefore, no other transformation product was detected during the dehalogenation of IPM in this work. In addition, the exact position of the iodine release could not be determined, and while the structures of the intermediates and products in Figure 1 are accurate in terms of the number of remaining iodine atoms, they are not necessarily in terms of their position at the aromatic ring. From an environmental standpoint, the reductive dehalogenated products are likely to be more biodegradable and less persistent (*28*), thus they could be effectively removed in a biological treatment process or in the receiving surface waters.

Application for the Treatment of Real Wastewater. As shown in Table 1, IPM was effectively removed from reverse osmosis concentrate at a granular graphite cathode of BESs, although the concentration of TOC was orders-of-magnitude higher than IPM in this waste stream. Moreover, the concentrations of TOC, COD, and color changed only slightly during the treatment at the granular graphite cathode of BESs. This demonstrates the high selectivity of the reductive dehalogenation of ICM in the electrochemical process. In addition, the estimated power required for IPM dehalogenation from reverse osmosis concentrate in a BES would be in the order of 0.05 kWh m^{-3} treated wastewater.

Electrode catalyst fouling and deactivation is a major challenge for electrochemical treatment processes in environmental matrices like wastewater effluent, due to the presence of natural organic matter. For example, a nickel electrode has to be activated daily by etching with dilute HCl and rinsing with deionized water (*9*). The granular graphite cathodes in this work have shown a long-term stability over at least three months for effective IPM removal from reverse osmosis concentrate without any electrode pretreatments or reactivation (Table 1). This could significantly simplify the operation and reduce the running costs for ICM removal from wastewater.

Results from this work demonstrate that a bioelectrochemical system is an effective and selective technology for dehalogenating ICM. Besides ROC wastewater, this BES technology could also have the potentials for pretreatment of hospital wastewaters that have IPM and other X-ray agents at higher concentrations (upper to mg L^{-1}) (*29*) before they are discharged to the sewage, as well as the groundwater with ICM concentrations in the upper ng L^{-1} range (*3*).

Acknowledgments

This research was supported by the Australian Research Council (Grant Nos. DP0985317, DP0666927, and LP0989159).

Supporting Information Available

Schematic of (A) continuous and (B) batch cathode experimental setup for IPM dehalogenation in BESs in Figure S1; experimental setup for granular graphite cathode in Table S1; UPLC-(+)ESI-MS extracted ion chromatograms (XIC) of full-scan chromatogram of reductively treated IPM solution in Figure S2; (+)ESI-QqLIT mass spectra for IPM and its products in Figure S3; proposed fragmentation pathway of IPM and its products in Figure S4; effect of (A) cathode pH and (B) DO concentration on IPM removal at the granular graphite cathode of BESs in Figure S5; IPM dehalogenation on a BDD cathode in BESs in Figure S6; and pseudo first-order rate constants for IPM dehalogenation at various cathode potentials in Figure S7. This information is available free of charge via the Internet at http://pubs.acs.org.

Literature Cited

(1) Seitz, W.; Weber, W. H.; Jiang, J. Q.; Lloyd, B. J.; Maier, M.; Maier, D.; Schulz, W. Monitoring of iodinated X-ray contrast media in surface water. *Chemosphere* **2006**, *64*, 1318–1324.

(2) Putschew, A.; Schittko, S.; Jekel, M. Quantification of triiodinated benzene derivatives and X-ray contrast media in water samples by liquid chromatography-electrospray tandem mass spectrometry. *J. Chromatogr. A* **2001**, *930*, 127–134.

(3) Ternes, T. A.; Hirsch, R. Occurrence and behavior of X-ray contrast media in sewage facilities and the aquatic environment. *Environ. Sci. Technol.* **2000**, *34*, 2741–2748.

(4) Steger-Hartmann, T.; Länge, R.; Schweinfurth, H. Environmental risk assessment for the widely used iodinated X-ray contrast agent Iopromide (Ultravist). *Ecotoxicol. Environ. Saf.* **1999**, *42*, 274–281.

(5) Pomati, F.; Castiglioni, S.; Zuccato, E.; Fanelli, R.; Vigetti, D.; Rossetti, C.; Calamari, D. Effects of a complex mixture of therapeutic drugs at environmental levels onhumanembryonic cells. *Environ. Sci. Technol.* **2006**, *40*, 2442–2447.

(6) Knitt, L. E.; Shapley, J. R.; Strathmann, T. J. Rapid metal-catalyzed hydrodehalogenation of iodinated X-ray contrast media. *Environ. Sci. Technol.* **2008**, *42*, 577–583.

(7) Stieber, M.; Putschew, A.; Jekel, M. Reductive dehalogenation of iopromide by zero-valent iron. *Water Sci. Technol.* **2008**, *57*, 1969–1975.

(8) Petersen, M. A.; Sale, T. C.; Reardon, K. F. Electrolytic trichloroethene degradation using mixed metal oxide coated titanium mesh electrodes. *Chemosphere* **2007**, *67*, 1573–1581.

(9) Zwiener, C.; Glauner, T.; Sturm, J.; Wörner, M.; Frimmel, F. H. Electrochemical reduction of the iodinated contrast medium iomeprol: iodine mass balance and identification of transformation products. *Anal. Bioanal. Chem.* **2009**, *395*, 1885–1892.

(10) Rozendal, R. A.; Hamelers, H. V. M.; Rabaey, K.; Keller, J.; Buisman, C. J. N. Towards practical implementation of bioelectrochemical wastewater treatment. *Trends Biotechnol.* **2008**, *26*, 450–459.

(11) Liu, H.; Grot, S.; Logan, B. E. Electrochemically assisted microbial production of hydrogen from acetate. *Environ. Sci. Technol.* **2005**, *39*, 4317–4320.

(12) Ren, Z. Y.; Ward, T. E.; Regan, J. M. Electricity production from cellulose in a microbial fuel cell using a defined binary culture. *Environ. Sci. Technol.* **2007**, *41*, 4781–4786.

(13) de Schamphelaire, L.; van den Bossche, L.; Dang, H. S.; Hofte, M.; Boon, N.; Rabaey, K.; Verstraete, W. Microbial fuel cells generating electricity from rhizodeposits of rice plants. *Environ. Sci. Technol.* **2008**, *42*, 3053–3058.

(14) Rabaey, K.; Van de Sompel, K.; Maignien, L.; Boon, N.; Aelterman, P.; Clauwaert, P.; De Schamphelaire, L.; Pham, H. T.; Vermeulen, J.; Verhaege, M.; Lens, P.; Verstraete, W. Microbial fuel cells for sulfide removal. *Environ. Sci. Technol.* **2006**, *40*, 5218–5224.

(15) Virdis, B.; Rabaey, K.; Yuan, Z.; Rozendal, R.; Keller, J. Electron fluxes in a microbial fuel cell performing carbon and nitrogen removal. *Environ. Sci. Technol.* **2009**, *43*, 5144–5149.

(16) Mu, Y.; Rozendal, R. A.; Rabaey, K.; Keller, J. Nitrobenzene removal in bioelectrochemical systems. *Environ. Sci. Technol.* **2009**, *43*, 8690–8695.

(17) Aulenta, F.; Reale, P.; Catervi, A.; Panero, S.; Majone, M. Kinetics of trichloroethene dechlorination and methane formation by a mixed anaerobic culture in a bio-electrochemical system. *Electrochim. Acta* **2008**, *53*, 5300–5305.

(18) Mu, Y.; Rabaey, K.; Rozendal, R. A.; Yuan, Z. G.; Keller, J. Decolourization of azo dyes in bio-electrochemical systems. *Environ. Sci. Technol.* **2009**, *43*, 5137–5143.

(19) Freguia, S.; Rabaey, K.; Yuan, Z.; Keller, J. Electron and carbon balances in microbial fuel cells reveal temporary bacterial storage behaviour during electricity generation. *Environ. Sci. Technol.* **2007**, *41*, 2915–2921.

(20) Rabaey, K.; Ossieur, W.; Verhaege, M.; Verstraete, W. Continuous microbial fuel cells convert carbohydrates to electricity. *Water Sci. Technol.* **2005**, *52*, 515–523.

(21) Greenberg, A.; Clesceri, L. S.; Eaton, A. D. *Standard Methods for Examination of Water and Wastewater*, 18th ed., Americal Public Health Association: WA, 1992.

(22) Dwyer, J.; Griffiths, P.; Lant, P. Simultaneous colour and DON removal from sewage treatment plant effluent: Alum coagulation of melanoidin. *Water Res.* **2009**, *43*, 553–561.

(23) Logan, B. E.; Hamelers, B.; Rozendal, R.; Schrorder, U.; Keller, J.; Freguia, S.; Aelterman, P.; Verstraete, W.; Rabaey, K. Microbial fuel cells: Methodology and technology. *Environ. Sci. Technol.* **2006**, *40*, 5181–5192.

(24) Mishra, D.; Liao, Z. H.; Farrell, J. Understanding reductive dechlorination of trichloroethene on boron-doped diamond film electrodes. *Environ. Sci. Technol.* **2008**, *42*, 9344–9349.

(25) Freguia, S.; Rabaey, K.; Yuan, Z. G.; Keller, J. Sequential anode-cathode configuration improves cathodic oxygen reduction and effluent quality of microbial fuel cells. *Water Res.* **2008**, *42*, 1387–1396.

(26) Cheng, I. F.; Fernando, Q.; Korte, N. Electrochemical dechlorination of 4-chlorophenol to phenol. *Environ. Sci. Technol.* **1997**, *31*, 1074–1078.

(27) Li, T.; Farrell, J. Reductive dechlorination of trichloroethene and carbon tetrachloride using iron and palladized-iron cathodes. *Environ. Sci. Technol.* **2000**, *34*, 173–179.

(28) Tunkel, J.; Howard, P. H.; Boethling, R. S.; Stiteler, W.; Loonen, H. Predicting ready biodegradability in the Japanese Ministry of International Trade and Industry test. *Environ. Toxicol. Chem.* **2000**, *19*, 2478–2485.

(29) Weissbrodt, D.; Kovalova, Ort.; Pazhepurackel, V.; Moser, R.; Hollender, J.; Siegrist, H.; McArdell, C. S. Mass flows of X-ray contrast media and cytostatics in hospital wastewater. *Environ. Sci. Technol.* **2009**, *43*, 4810–4817.

ES1022812